JOURNAL OF GENERAL VIROLOGY

RESEARCH ARTICLE

Jaccard *et al.*, *Journal of General Virology* 2023;104:001879

DOI 10.1099/jgv.0.001879

MICROBIOLOGY SOCIETY

New viruses of *Cladosporium* sp. expand considerably the taxonomic structure of *Gammapartitivirus* genus

Augustine Jaccard, Nathalie Dubuis, Isabelle Kellenberger, Justine Brodard, Sylvain Schnee, Katia Gindro and Olivier Schumpp*

Abstract

Despite the fact that *Cladosporium* sp. are ubiquitous fungi, their viromes have been little studied. By analysing a collection of *Cladosporium* fungi, two new partitiviruses named Cladosporium cladosporioides partitivirus 1 (CcPV1) and Cladosporium cladosporioides partitivirus 2 (CcPV2) co-infecting a strain of *Cladosporium cladosporioides* were identified. Their complete genome consists of two monocistronic dsRNA segments (RNA1 and RNA2) with a high percentage of pairwise identity on 5′ and 3′ end. The RNA directed RNA polymerase (RdRp) of both viruses and the capsid protein (CP) of CcPV1 display the classic characteristics required for their assignment to the *Gammapartitivirus* genus. In contrast, CcPV2 RNA2 encodes for a 41 KDa CP that is unusually smaller when aligned to CPs of other viruses classified in this genus. The structural role of this protein is confirmed by electrophoresis on acrylamide gel of purified viral particles. Despite the low percentage of identity between the capsid proteins of CcPV1 and CcPV2, their three-dimensional structures predicted by AlphaFold2 show strong similarities and confirm functional proximity. Fifteen similar viral sequences of unknown function were annotated using the CcPV2 CP sequence. The phylogeny of the CP was highly consistent with the phylogeny of their corresponding RdRp, supporting the organization of *Gammapartitiviruses* into three distinct clades despite stretching the current demarcation criteria. It is proposed that a new subgenus be created within the genus Gammapartitivirus for this new group.

INTRODUCTION

A large number of different micro-organisms, such as filamentous fungi, yeasts, viruses or bacteria naturally colonise the vine [1, 2]. These organisms, collectively known as the plant microbiome, develop interactions with each other and with their host, all contributing to the functioning and evolution of a discrete ecological entity referred to as the holobiont [3–7]. These interactions can influence plant growth, response to pathogens, metabolite productions and adaptation to environmental changes [1, 8].

The holobiont protagonists combine different levels of interaction: the presence of viruses infecting fungal endophytes, so-called mycoviruses, may sometimes favour the development of the host plant with potentially interesting agronomical consequences. Seminal work has demonstrated the role of the mycovirus Cryphonectria hypovirus one in reducing the virulence of *Cryphonectria parasitica,* the fungus responsible for chestnut blight fungus [9, 10]. A more recent study showed that the mycovirus Sclerotinia sclerotiorum hypovirulence-associated DNA virus one down-regulates pathogenicity factors of its fungal host, *Sclerotinia sclerotiorum*, resulting in a reduction of fungal virulence and conferring beneficial endophytic properties that stimulates plant growth and response to stress [11]. Hence, mycoviruses appear as putative solutions for plant protection especially for vine cultivation that requires quantities of phytosanitary products with a strong impact on natural ecosystems. These mycoviruses are particularly abundant in the grapevine, where their great diversity has been revealed by high-throughput sequencing analyses [12–14]. The interactions between grapevines and their endophytic fungal communities are complex, and the role of mycoviruses detected in the fungal strains that make up these fungal communities is a second level of interaction

Received 13 June 2023; Accepted 25 July 2023; Published 07 August 2023
Author affiliations: [1]Department of Plant Protection, Agroscope, Nyon, Switzerland.
***Correspondence:** Olivier Schumpp, olivier.schumpp@agroscope.admin.ch
Keywords: Cladosporium; Gammapartitivirus; mycovirus; taxonomy; VANA.
Abbreviations: CcPV1, cladosporium cladosporioides partitivirus 1; CcPV2, cladosporium cladosporioides partitivirus 2; CP, capsid protein; HP, hypothetical protein; ICTV, International Committee on Taxonomy of Viruses; LC-MS/MS, liquid chromatography tandem mass spectrometry; RdRp, RNA directed RNA polymerase; SDS-PAGE, sodium dodecyl sulfate-polyacrylamide gel electrophoresis; VANA, virion-associated nucleic acids.
One supplementary figure and five supplementary tables are available with the online version of this article.

that is very poorly understood. As a result, no mycovirus has yet been identified to manage fungal diseases in grapevine or to enhance plant resistance to abiotic stresses.

Cladosporium, one of the largest genera of dematiaceous fungi present in the environment, is also dominant as grapevine endophyte [15–17]. Its presence on leaves and berries increases progressively with the growing season [18] and late harvesting can favour the development of Cladosporium rot on the berries (*C. cladosporioides* and *C. herbarum*) which affects wine quality [19]. We analysed the prevalence and genome structures of viruses of this ubiquitous fungal species to understand better their role and the possible exchanges of viruses within strains composing vine fungal communities.

An approach based on the extraction of virion-associated nucleic acids (VANA), originally adapted for plant viruses, has proved highly effective on fungal mycelium. Four genomic segments forming two *Partitivirus* coexisting in *Cladosporium cladosporiodes* were identified and characterized.

This work enabled us to assign a structural function to 15 hypothetical viral proteins that form a distinct clade in the genus *Gammapartitivirus*. It includes viruses with a novel capsid protein sequence showing very little similarities to the capsid protein sequences of any other *Gammapartitivirus*.

METHODS

Fungal isolates

The fungal community was isolated from sap bleedings collected on an Agroscope experimental plot at Leytron (VS, Switzerland). The sap was collected in 50 ml brown glass bottles. Bottles were sterilized with ethanol, sealed with parafoil and left for 2 weeks during the bleeding season. Then 100 µl of sap sample diluted one hundred times with sterile water were plated on Potatoes Dextrose Agar with aureomycin 12 mg l^{-1} (PDAa). Fungi were isolated by subculture of emerging mycelium on PDA petri dishes. In total, 249 fungal isolates were cultured from the grapevine bleeding sap of 41 vinestocks. A visual classification based on the morphology of the colonies revealed a predominance of *Cladosporium* and *Aureobasidium* as previously reported on grapevines [16, 18]. To avoid the analysis of individuals from the same lineage, only one isolate of each genus was selected per plant. Their identity was confirmed by ITS sequencing of a representative isolate using ITS1F/ITS4 primer as previously described [20]. Twenty-two *Aureobasidium* isolates, 14 *Cladosporium* isolates and 12 isolates representing the diversity of colony morphotypes were selected for virus screening.

Following the identification of a virus in a *Cladopsorium* strain, 12 *Cladopsorium* isolates present in Agroscope's fungal collection (https://www.mycoscope.ch/) were further screened by RT-PCR for the presence of this virus.

Semi-purification of virus particles

Particle purification was performed according to a previously-described protocol with some modifications [21]. Briefly, 15–30 g of fresh mycelium from Potatoes Dextrose Agar culture were ground into small powder using liquid nitrogen and a mixer (Sorvall Omni Mixer 17 150 Homogenizer). The powder was supplemented with 6 vol of extraction buffer (0.5 M Tris, pH 8.2, 5% v/v Triton, 4% v/v Polyclar AT, 0.5% w/v bentonite, 0.2% v/v β-mercaptoethanol) and stirred on ice. After 20 min of homogenisation, the suspension was filtered through a double layer of cotton cloth. About 120 ml of filtrate was centrifuged at 4500 ***g*** for 20 min. The supernatant was then collected and placed on 5 ml of 20% sucrose cushion (diluted in 0.1 M Tris, pH 8.2) followed by centrifugation at 150000 ***g*** using a Beckman Coulter 45Ti rotor for 1.5 h. The resulting pellet was incubated overnight at 4 °C in 1 ml of suspension buffer (0.02 M Tris, pH 7.0, 0.001 M $MgCl_2$). Enrichment in viral particles was verified by electron microscopy using 3 µl of particles as previously described [22], using the Tecnai G2 Spirit microscope (FEI, Eindhoven).

RNA extraction

Total RNA extraction from fungal field isolates sub-cultured on agar plates was carried out according to Akbergenov *et al.* [23] with the following modifications: 0.5 cm^2 square of mycelium (50–100 mg) was cut from the edge of the plate with a scalpel, and placed in a 1.5 ml Eppendorf tube with three 3 mm glass beads and frozen in liquid nitrogen. The grinding was carried out by shaking the tubes in a Tissuelyser (Qiagen) for 60 s at 30 Hz. If necessary, the operation was repeated once after incubation in liquid nitrogen. Then 1 ml of extraction buffer (6.5 M Guanidine hydrochloride; 100 mM tris HCL pH=8; 100 mM β-mercaptoethanol) was added to the tube and mixed. The samples were incubated at room temperature for 10 min and then centrifuged for 10 min at 13300 ***g*** at 4 °C. The supernatant was transferred to a 2 ml Eppendorf tube. After the addition of 0.5 ml of Trizol (Invitrogen) reagent and 0.2 ml of chloroform, tubes were centrifuged 10 min at 13300 ***g***. The upper phase was transferred to a RNase-free 50 ml polypropylene Beckman Bottles, supplemented with an equivalent volume of isopropanol, and incubated on ice for 30 min. The tube was centrifuged for 20 min at 13300 ***g*** at 4 °C. The pellet was washed in 70% ethanol, dried at room temperature, resuspended in 30 µl H_2O and stored at −80 °C.

VANA from the Agroscope's fungal collection isolate *C. cladosporioides* AGS-1338 grown on PDA medium were extracted according to the protocol initially adapted for plant virus described in [24, 25]. Briefly, 200 µl of semi-purified particles described

above were treated with 1 µl of DNAse and 1 µl of RNAse (Euromedex) for 90 min at 37 °C to remove non-encapsulated RNA and DNA as described previously by Maclot *et al.* [26]. Subsequently, 400 µl of lysis buffer from the RNeasy plant mini kit (Qiagen) and 60 µl of N-Laurylsarcosine sodium salt solution 30% were added and mixed by gentle agitation at 70 °C for 20 min. Then 500 µl of the solution were loaded on a QIAshredder spin column and further processed according to manufacturer's recommendation.

Library preparation, sequencing and bioinformatic analyses

Total RNA extracted from 22 isolates from *Aureobasidium* sp., 14 isolates from *Cladosporium* sp. and 12 isolates representing other fungal species were pooled with equal quantity and treated for DNase with the RNase-Free DNase Set (Qiagen). RNA quality was controlled with a BioAnalyzer (Agilent Technology). A final extract of approximately 2.6 µg was used for the preparation of the cDNA library. mRNA library preparation was performed with TruSeq Stranded mRNA kit. cDNA for mRNA were sequenced using an Illumina NextSeq High library preparation kit and sequenced on an Illumina NextSeq 550 System (Illumina, USA) in paired-end 2×75 nt reads by Fasteris (Genesupport, Switzerland). Raw reads were trimmed with BBDuk 37.64 plugin and assembled using SPAdes plugin in Geneious Prime 2019.0.4 [27, 28].

Synthesis of the cDNA and tagged-library preparation from VANA was performed as described by Candresse *et al.* [24] using TruSeq DNA Nano kit. Library quality was controlled using a Bioanalyzer 2100 and sequenced at Fasteris (Genesupport, Switzerland) on Miseq nano kit version 2 (Illumina, USA) in 1×50+8+8 cycles. Reads trimming was carried out using BBDuk 38.37 plugin from Geneious Prime 2020.0.4 (Biomatters, Auckland), and *de novo* assembly was performed using parameters of the high sensitivity mode from Geneious assembler.

Reconstruction of whole genomic sequences and annotation

Contigs were selected and annotated using blastn on a 'in-house' mycovirus database including viral genera of previously described mycoviruses, prepared from refseq sequences present in NCBI (01.05.2020). Reads were mapped to reference sequences identified by blast and primers were designed on reads stacks to confirm the sequence of each contig by Sanger sequencing and reconstruct the full genomes by RACE PCR (Table S1). AMV reverse transcriptase (Promega, Switzerland) and GoTaq polymerase (Promega, Switzerland) were used for a one-step protocol. RT-PCR cycling conditions were 45 min at 48 °C, followed by 2 min at 94 °C, then 35 cycles of 45 s at 94 °C, 40 s at 55 °C and 1.5 min at 72 °C, ended by 10 min at 72 °C. A denaturing step was applied according to Asamizu *et al.* [29] before using the SMARTer RACE 5′/3′ Kit (5′ section only) according to manufacturer's recommendations. Amplified RACE and RT-PCR products were cloned in pGEM-T, sequenced and assembled using Geneious assembler with highest sensitivity parameters. Reads were mapped on the assembled sequences to control the assembly. An extra stretch of seven nucleotides (ACATGGG) detected in all RACE sequences but not described in the kit specification was removed.

The annotation of the selected contigs was verified by online blastn and blastx analysis. The presence and size of an Open Reading Frame (ORF) was predicted for each segment by ORF finder (ncbi.nlm.nih.gov/orffinder).

Viral particles characterisation

Virus particles were concentrated with a 10–40% sucrose gradient prepared with a Buchler gradient maker (Buchler Instruments Inc., Fort Lee, NJ, USA) with 17.5 ml of 10% (v/v) and 17.5 ml of 40% (v/v) sucrose in the suspension buffer (0.02 M Tris, pH 7.0, 0.001 M $MgCl_2$). One millilitre of virus particles was overlaid on the sucrose gradient and ultracentrifuged for 2.5 h at 150000 ***g*** at 4 °C using a Beckman Coulter SW32Ti rotor. After centrifugation, fractions of 1.8 ml from top to bottom were collected and numbered from #1 to #20. Groups of three fractions were pooled, diluted in 40 ml of suspension buffer and centrifuged 2.5 h at 180000 ***g*** using a Beckman Coulter 50.2Ti rotor. The pellet was suspended in 200 µl suspension buffer. Fraction groups #10 to #12, #13 to #15 and #16 to #18 were visualized by TEM. Particles from fraction #13 to #15 were used to measure the diameter of particles with ImageJ [30]. The calculation of the mean, standard deviation and the mean comparison with a student t-test was performed in R.

LC-MS/MS

The semi-purified particles were loaded onto a 12% (v/v) sodium dodecyl sulfate-polyacrylamide gel electrophoresis (SDS-PAGE) gel. A 100 kDa size marker was used for size estimation (Biorad, low range standards). After electrophoresis, the gel was stained with Coomassie brilliant blue R250. The resulting band of the expected size of the putative capsid of CcPV1 and CcPv2 were excised and subjected to mass spectrometry coupled to liquid chromatography (LC-MS/MS) analysis at the Centre for Integrative Genomics (University of Lausanne, Switzerland) for determination of protein sequence.

Annotation and phylogenetic analysis

The protein sequences encoding for RdRp and CP identified in this work were aligned with the protein sequences of members of the family *Partitiviridae* available from ICTV website and other members of newly described zeta and epsilon genera [31, 32] (Table S2). The Human picobirnavirus strain Hy005102 reference sequence was used as an outgroup of the RdRp tree. Alignment

was performed using MUSCLE version 3.8.425 implemented in Geneious Prime 2020.0.4 with standard parameters [33]. The resulting alignment quality was verified manually and zones with alignment ambiguities were excluded for tree and distance matrix calculation. The phylogenetic tree was reconstructed with IQ-tree, using the optimised model for maximum likelihood method [34, 35]. Branching support was obtained with 1000 boostraps with the ultrafast method from IQ-Tree [36]. The phylogenetic trees were curated on iTol [37].

Research for protein domains was done with CDsearch of NCBI in the pfam database [38] and annotation of the sequence was done with ORF finder from NCBI to identify the proper coding region of the sequence.

RESULTS

Virus identification

Despite the elevated number of reads and contigs generated by Illumina sequencing of pooled fungal RNA prepared from 48 isolates collected in Leytron, only one viral contig of 123 bp could be confirmed by RT-PCR. This contig was identified in the *C. ramotenellum* strain AGS-Cb3.2 only (Fig. S1A). A fragment of 101 bp was amplified with the primer set 10/89 and shared 93% identity with the NCBI sequence MN034127 reconstructed from a soil metagenome study annotated as a *Partitiviridae* sp. [39]. In the absence of reverse transcription, no amplification was observed confirming the viral replicative nature of the fragment.

New primers (193/1035) designed on the sequence MN034127 enabled the amplification of a longer fragment of 1218 nucleotides that led to the complete genomic fragment reconstruction by RACE-PCR from AGS-Cb3.2. Read mapping on this complete sequence showed that only 15 reads covering 13% of the sequence mapped on this sequence with 100% identity. The infected AGS-Cb3.2 strain could not be maintained.

Twelve *Cladosporium* isolates maintained in the Agroscope fungal isolate collection (https://mycoscope.bcis.ch/) were then screened by RT-PCR using the primer 10/89. The *C. cladosporioides* strain AGS-1338 isolated from a vine stock of Chasselas in 2010 in Perroy (VD, Switzerland) produced a band corresponding to the expected viral fragment size, and the viral sequence was confirmed with Sanger sequencing of the purified band (Fig. S1B, available in the online version of this article). The identity of the fungal isolate was confirmed by sequencing and blastn analysis of the ITS sequence.

Mycovirus genomes reconstruction

A second Illumina sequencing was performed using the *C. cladosporioides* isolate AGS-1338 to reconstruct the complete genome of the virus previously detected in AGS-Cb3.2, especially the second genomic fragment of this virus whose affiliation to the *Partitiviridae* family required a bisegmented genome [40]. The sequencing strategy was based on a protocol initially adapted for plant virus using VANA instead of total RNA extracts [24]. Four contigs were significantly longer with sizes of 1629, 1953, 1980 and 2139 bp. RT-PCR with primers designed on these four contigs confirmed their presence in the strain AGS-1338. Read mapping on these four contigs showed a depth of coverage of 139 to 559 reads on average, with maximums of 311 to 1548 reads depending on the fragment. Coverage dropped sharply at the end of the fragments to 1–4 reads, suggesting trimming or sequencing errors. The exact 5′ and 3′ ends of each fragment were determined with RACE-PCR, and the full genome sequences were confirmed by Sanger sequencing. Final sequences were smaller than those obtained by the bioinformatics analysis of Illumina reads with sizes of 1356, 1586, 1771 and 1705 nucleotides (Fig. 1a). These sequences were covered by 33.3, 21, 12.4 and 27.4% of the total reads obtained by Illumina sequencing, respectively.

A blastn and blastx analysis of the four contigs identified two sequences coding for RdRp (Contig1 and 3) one CP (Contig2) and a Hypothetical Protein (HP, Contig4, Fig. 2). The four sequences did not have a poly-A tail and showed a GC content between 45.1 and 52.7%, which corresponded to the average GC content values for dsRNA viruses in general including *Partitiviridae* [41]. An RT-like super family conserved domain was detected on Contig1 and 3 using CDsearch. The same analysis performed on the sequence reconstructed from *C. ramotenellum* strain AGS-Cb3.2 lead to the identification of a unique ORF encoding a RdRp (Contig1-Cb3.2) (Fig. 1a).

All segments were more than 90% identical to one or more viral segments assigned to the *Partitiviridae* family. *Partitiviridae* are multisegmented viruses, composed of two segments encoding for a RdRp (RNA1) and a CP (RNA2) [40]. This genomic organisation was confirmed for all four sequences by the analysis of the fragment ends. Contig1-1338 and Contig2-1338 termini showed a high sequence identity on both 5′ and 3′ ends, thereby confirming these two genomic fragments encoding for an RdRp (RNA1) and a CP (RNA2) were forming the complete genome of a virus (Fig. 1b). Contig1 and 2 were covered with the approximate same number of reads (Fig. 2).

The UTR of the Contig3-1338 and Contig4-1338 also showed high sequence identity: they shared a common stretch of six identical nucleotides at the 5′ end and a long stretch of 71 identical nucleotides at the 3′ (Fig. 1b). Contig3-1338 encoded for a RdRp. As shown by protein sequencing (see results below), the Contig4-1338 encoded for a so far undescribed CP type. Contig3 and 4 were also covered with the approximate same number of reads (Fig. 2). Thus, we concluded that both fragments corresponded to

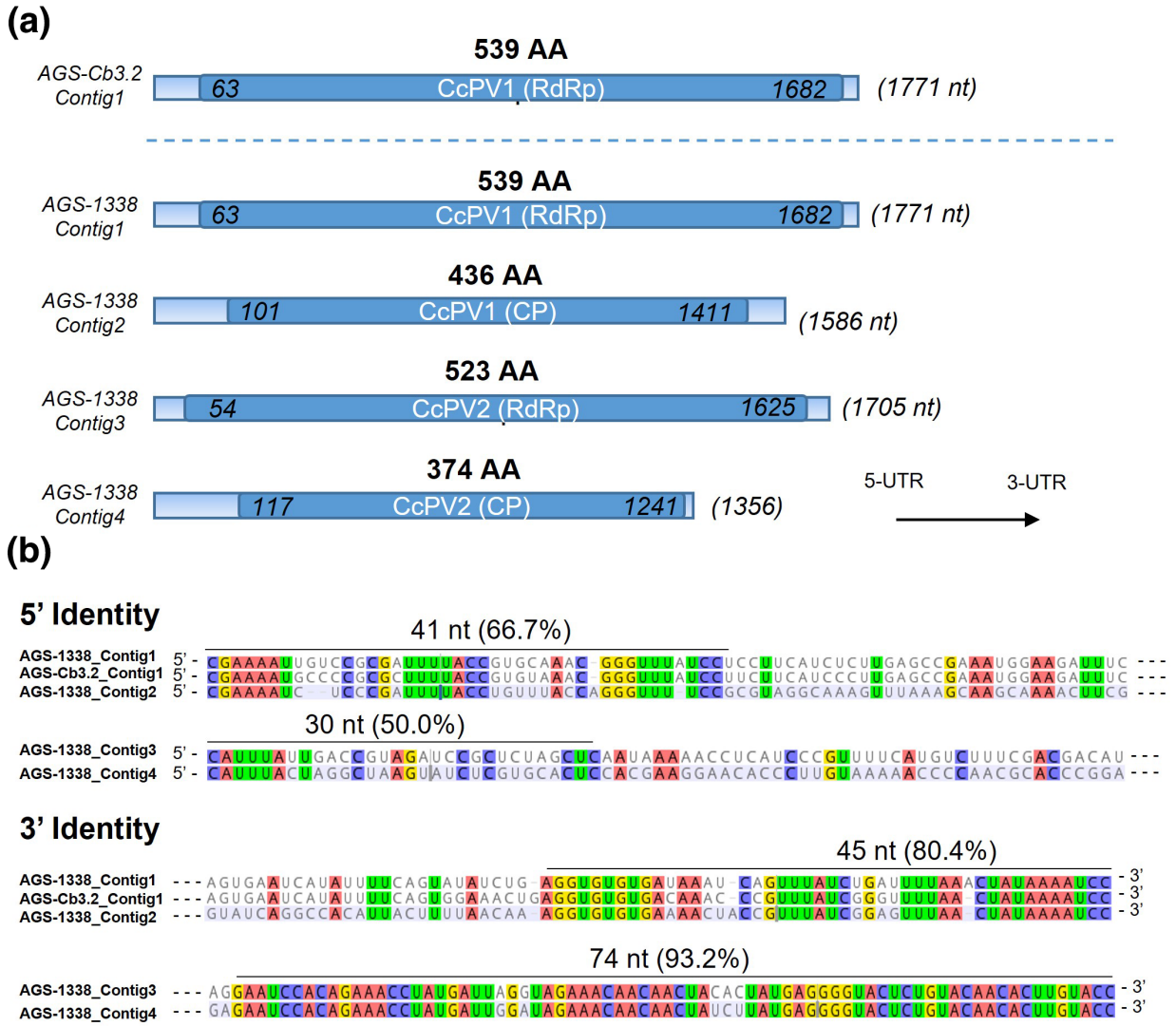

Fig. 1. Characteristic of the sequences of CcPV1 and CcPV2 detected in strain *C. cladosporioides* AGS-1338 and *C. ramotenellum* Cb3.2. (a) Viral contigs. Coding sequences are highlighted in dark blue and the 5'- and 3'-UTRs sequences in light blue. Nucleic acid position of the start and end of the ORF is indicated. The size of the full nucleic sequence is in brackets. (b) Alignment of the 5'- and 3'-UTRs of the genomic segments present in isolates AGS-1338 and AGS-Cb3.2. Nucleotides shared among the different sequences are highlighted and the percentage of identity of the most conserved parts is indicated.

the RNA1 and RNA2 of a second virus infecting infecting AGS-1338. These two viruses are close to viral sequences derived from metagenomic work which are referred to as 'associated' with uncultivable fungal species or with lesions produced by uncultivable fungal species infecting grapes. In view of the ubiquitous nature of *Cladosporium*, very common on grapes, we consider this assignment to be uncertain. In contrast, in our work, both viruses were identified from a *Cladosporium* isolate in pure culture identified by sequencing and maintained in a collection. They were verified by full-length sequencing. For all these reasons, we provisionally named these viruses Cladosporium cladosporioides partitivirus 1 and 2, respectively, and hereafter refer to them as CcPV1 and CcPV2.

Virion characterisation and CP sequencing

Particles enrichment by ultra-centrifugation was verified by TEM. Two types of particles could be observed (Fig. 3b). Large dense spherical particles of 36.2±2.6 nm (n=25) with a contrasted outline distinguished from smaller bright spherical particles of 31.5±2.4 nm (n=24) in AGS-1338 hosting CcPV1 and CcPV2. A t-test supported the size difference (p.value=4.3e-8; Table S3).

Occasionally, the concentration of CcPV1 in some plate subcultures was lower. Drawn on this finding, particle enrichments from two subcultures presenting high and low viral titre of the CcPV1 but same titre of CcPV2 were prepared (Fig. 3). Protein separation

(a)

Contigs	Contig length (nt)	Mapped reads	Protein function	Bests hit identification (blastx)	Accession number	Query cover (%)	Identity (%)	E.value
Contig1-1338	1771	2207	RdRp	Erysiphe necator associated partitivirus 3	GJW70322.1	90%	92%	0E+00
				Erysiphe necator associated partitivirus 2	GJW70319.1	90%	90%	0E+00
Contig2-1338	1586	2154	CP	Plasmopara viticola lesion associated Partitivirus 3	QHD64799.1	81%	100%	0E+00
				Erysiphe necator associated partitivirus 3	QJW70321.1	81%	86%	0E+00
Contig3-1338	1705	4857	RdRp	Plasmopara viticola lesion associated Partitivirus 4	QHD64807.1	89%	99%	0E+00
				Plasmopara viticola lesion associated Partitivirus 3	QHD64801.1	88%	77%	0E+00
Contig4-1338	1356	5908	HP	Plasmopara viticola lesion associated Partitivirus 4	QHD64811.1	81%	97%	0E+00
				Colletotrichum gloeosporioides partitivirus 1	QED88096.1	81%	66%	1E-173

(b)

ORF	Contig length (nt)	Mapped reads	Protein function	Bests hit identification (blastn)	Accession number	Query cover (%)	Identity (%)	E.value
Contig1-1338	1771	2207	RdRp	Plasmopara viticola lesion associated Partitivirus 10	MN556983.1	91%	94%	0E+00
				Partitiviridae sp.	MN035614.1	96%	91%	0E+00
Contig2-1338	1586	2154	CP	Plasmopara viticola lesion associated Partitivirus 3	MN556982.1	98%	98%	0E+00
				Erysiphe necator associated partitivirus 3	MN605495.1	97%	84%	0E+00
Contig3-1338	1705	4857	RdRp	Plasmopara viticola lesion associated Partitivirus 4	MN556990.1	89%	96%	0E+00
				Hangzhou partiti-like virus 1	OM514386.1	88%	73%	0E+00
Contig4-1338	1356	5908	HP	Plasmopara viticola lesion associated Partitivirus 4	QHD64811.1	81%	97%	0E+00

Fig. 2. Blast annotation for the four viral segments identified in AGS-1338. (a) Blastx annotation, (b) Blastn annotation.

performed on SDS-PAGE showed two bands of about 47 and 41 kDa in the culture CcPV1^{+}/CcPV2^{+} with high viral titre of both viruses, corresponding to the calculated size of the ORF from RNA 2 of CcPV1 annotated as a CP and the calculated size of the ORF from RNA 2 of CcPV2 initially annotated as HP, respectively (Fig. 3b). However, no band of 47 KDa was observed in the culture CcPV1^{-}/CcPV2^{+} with low viral titre of CcPV1, indicating that the missing p47 was indeed the CP of CcPV1 (Fig. 3c). LC-MS/MS analysis yielded 34 unique peptides covering 83% CP of CcPV1 for the p47 protein while p41 protein sequencing yielded 26 unique peptides covering 79% of the ORF of RNA 2 of CcPV2. These results demonstrated that the Contig4-1338 was a capsid protein and was therefore referred to as CP of CcPV2.

AlphaFold2 was used to predict the secondary and 3D structure of the CPs of CcPV1 and CcPV2, yielding five different predictions for each protein (not shown). Protein sections predicted with high AlphaFold confidence showed marginal differences between the five different predictions. Comparison of the two proteins using icn3D [42] showed that despite low amino acid sequence similarity, the two proteins share very similar secondary structures in some regions, resulting in similar 3D structures, confirming that they are functionally related (Fig. 4).

Phylogenetic analysis

The two RdRp and CP sequences were aligned with protein sequences from representative members of the *Partitiviridae* family currently accepted by ICTV. The list was completed by viruses identified by blastx analysis of the CP for which RdRp was also available (Table S2).

The phylogenetic trees of both RdRps and CPs assigned CcPV1 and CcPV2 in the *Gammapartitivirus* genus. Both trees allowed the distinction of three subclades, named I, II and III, and showed a high degree of consistency for all but two viruses. Plasmopara viticola lesion associated Partitivirus 3 (PvlaPV3) had a RdRp grouped in clade III and a CP in clade II. Ustilaginoidea virens partitivirus (UvPV) is an interesting case discussed in greater detail below. Its RdRp and its CP grouped in clade II, but this virus was associated with a third protein that clustered in clade III. In both trees, CcPV1 clustered in the sub-group II and CcPV2 in clade III (Fig. 5).

The RdRp identified in AGS-Cb3.2 had over 92% amino acid identity with the CcPV1 RdRp. Despite the lack of detection of a CP in AGS-Cb3.2, this high level of identity confirmed that the viral sequence detected in AGS-Cb3.2 corresponded to another isolate of CcPV1, present in another species of *Cladosporium*.

The RdRp of CcPV2 clustered in the *Gammapartitivirus* genus with strong statistical support. However, the percentage of amino acid sequence identity falls under the 24% threshold required to delineate the *Partitiviridae* genus in pairwise comparisons with viruses of the clade I [40] (Fig. 5b, Table S5). The length of the RNA two encoding for the CP was 1356 nt that is 89 nt below the 1445 to 1611 nt range that are observed in species of the *Gammapartitivirus* genus. Similarly, the length of the CP of CcPV2 (374 AA) and all viruses of group III were also well below the 413–443 AA length of the CPs of viruses belonging to the genus *Gammapartitivirus*.

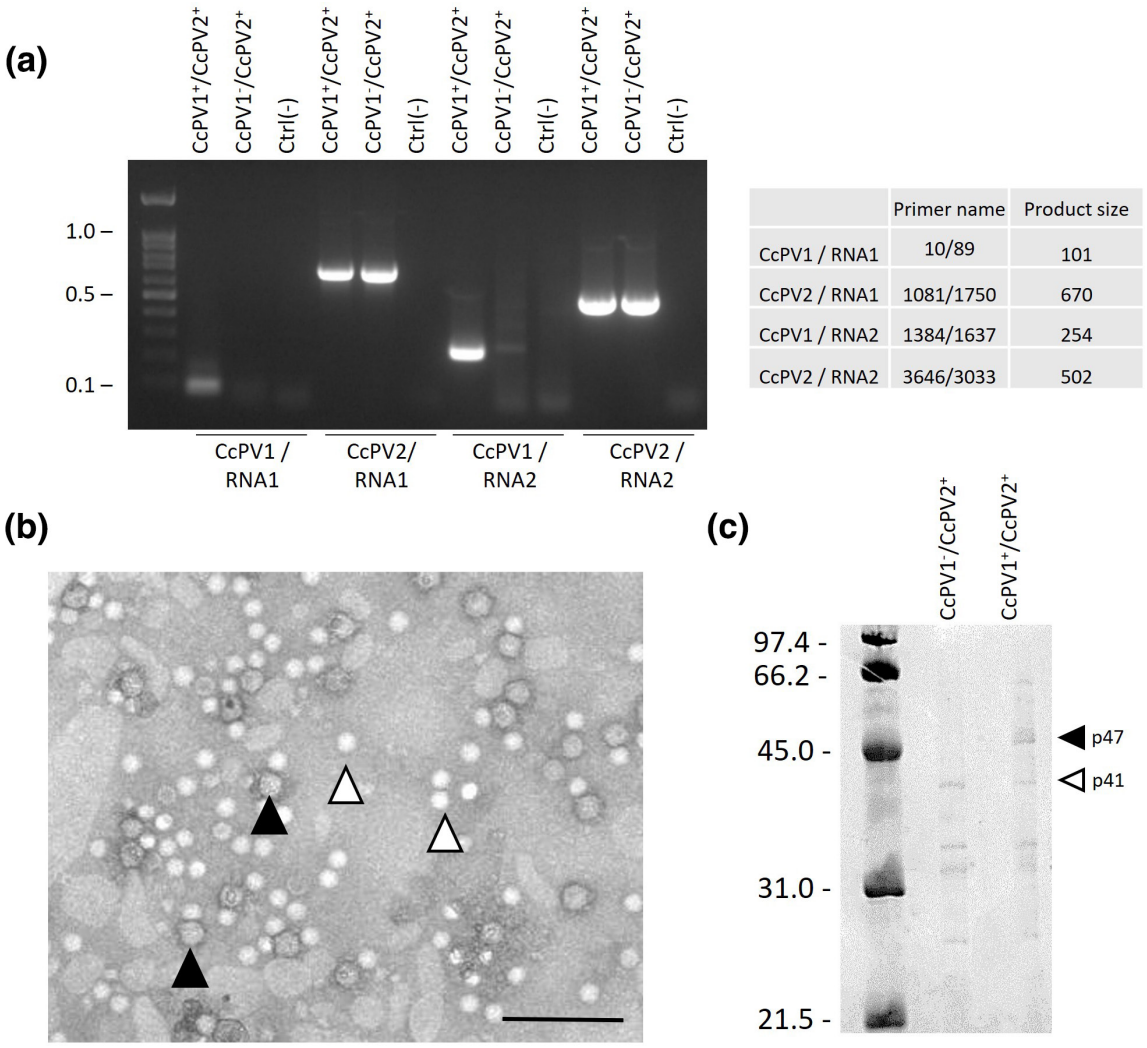

Fig. 3. Analysis of the viral particles of *C. cladospirioides* AGS-1338. (a) RT-PCR of two sub-culture of AGS-1338. DNA ladder is 100 bp. (b) TEM of semi-purified viral particles from *C. cladospiroides* AGS-1338. Black arrows designate larger viral particles. White arrow designates smaller viral particles. Scale bar represents 200 nm. (c) SDS-PAGE of semi-purified virus particles from CcPV1$^+$/CcPV2$^+$ and CcPV1$^-$/CcPV2$^+$ subcultures. Electrophoresis gel was stained with Coomasie blue.

In line with these results, the calculated weight of the CP of viruses from clade III were of 40–42 KDa, close to the 41 KDa of the CP from CcPV2. This contrasted with the calculated weight of 46–48 KDa of the CP of viruses currently accepted by ICTV clustering in clade I and II. Finally, these results were also consistent with the particle sizes that could be measured: Penicillium stoloniferum viruses S (PsV-S), having particles of about 35 nm in diameter [43] was grouped in clade II with CcPV1 which had a particle size of 36.2 nm in diameter while CcPV2 having particle size of 31.5 nm in diameter was assigned to clade III.

DISCUSSION

High-throughput sequencing analyses revealed the presence of numerous mycoviruses representing a wide diversity of viral families in grapevine [12, 17]. Many examples of mycoviruses demonstrate their capability of altering the virulence of plant pathogenic fungi [44–46] and others promote fungal growth and/or sporulation [47–49]. However, despite some exceptions, some viral families that are very common in filamentous fungi such as the *Partitiviridae* are less frequently associated with a fungal phenotype [46, 50–52].

This apparent lack of phenotype raises questions about the role of these viruses in the development cycle of their fungal host. In order to understand better virus-fungus interactions, the aim of this study was to characterise the virome of fungal communities from grapevine wood. *Cladosporium* sp. are known to be highly represented in grapevine fungal communities and are also

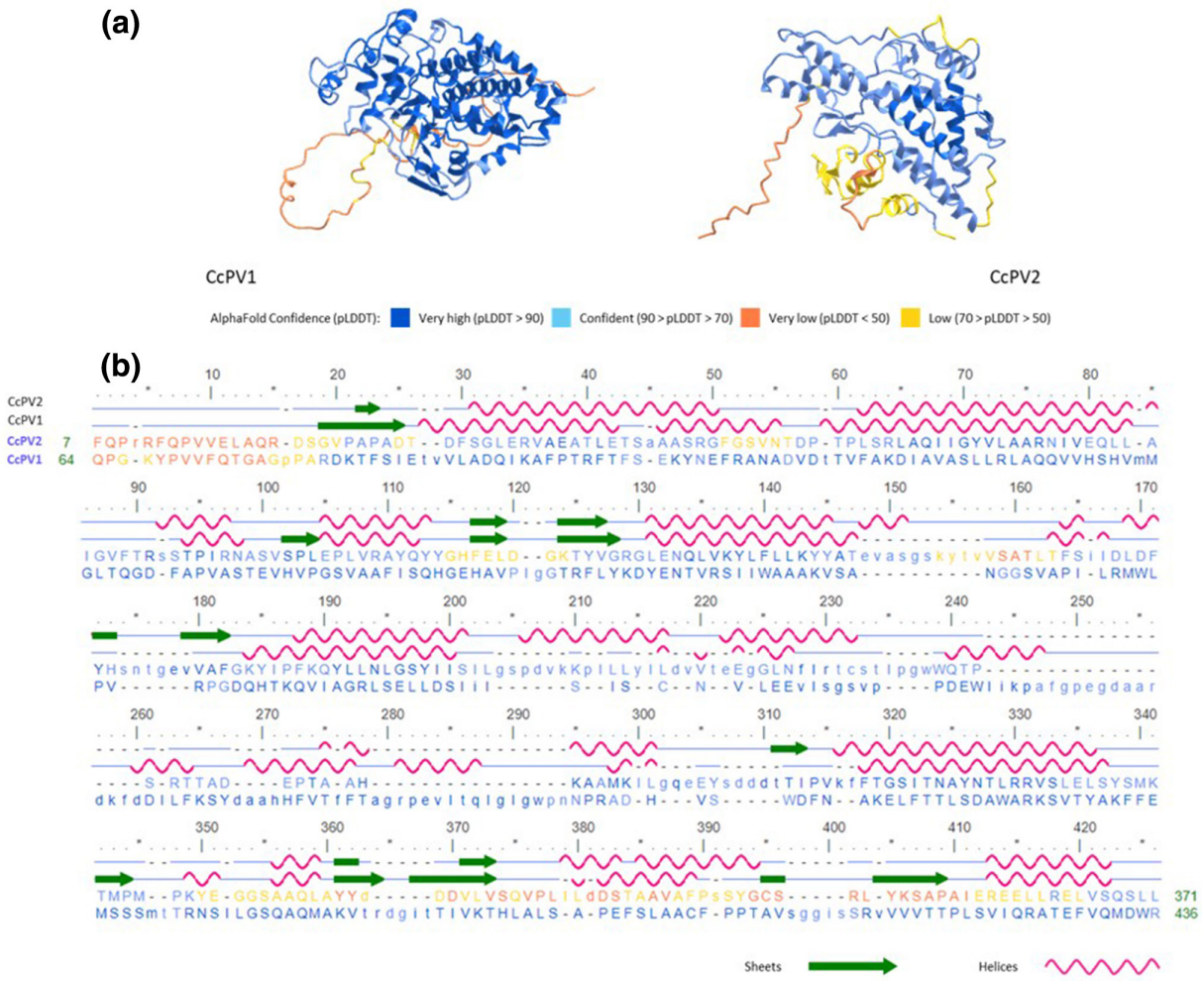

Fig. 4. AlphaFold2 structural predictions. (a) Representative 3D predictions for CcPV1 and CcPV2 capsids. (b) Secondary structures along the amino acid sequence of the two protein structures of CcPV1 and CcPV2. α-Helices are pink and *β*-sheets are indicated by green arrows. Colour of 3D structure (a) and amino acid chains (b) determined by confidence level of Alphafold2 prediction.

widespread in most ecological niches [17, 53]. This partly explains the large number of *Cladosporium* virus sequences in the NCBI databases. Nevertheless, these sequences are mainly derived from metagenomic work and form incomplete genomes in the vast majority of cases. Consequently, only seven complete viral genomes from cultivated isolates have been described to date [17, 54]. In this work, we carefully reconstructed and characterised the complete genomes of CcPV1 and CcPV2, two new mycoviruses detected in *Cladosporium* strains isolated from grapevine fungal communities. The presence of these mycoviruses was evaluated in a collection of *Cladosporium* isolates. To our knowledge, this is the first study specifically targeting *Cladosporium* isolates in pure cultures isolated from grapevine fungal communities.

Only one small contig corresponding to a viral RdRp sequence of partitiviridae could be identified and confirmed by RT-PCR in a single fungal isolate (Cb3.2) of the *C. ramotenellum* species. The strain *C. ramotenellum* Cb3.2 declined rapidly and could not be maintained in collections or in liquid culture. Senescence phenomena are common in many fungal species [55, 56] and in some cases the role of a mycovirus in reducing the life span of fungal species could be demonstrated [57]. However, a stable strain of *C. cladosporioides* AGS-1338 maintained at Changins for 12 years was also infected with this mycovirus, suggesting that this viral species is not the cause of the decline of its fungal host. Thus, as for most *Partitiviridae* described so far, this mycovirus does not appear to have a negative effect on the long-term survival of its fungal host.

The sensitivity of mycovirus detection was drastically improved using a VANA enrichment from liquid culture. Four genomic segments with good coverage were identified after sequencing the VANA. None of these segments could be detected by RT-PCR in any other isolate but the RdRp of CcPV1 in isolate Cb3.2 only.

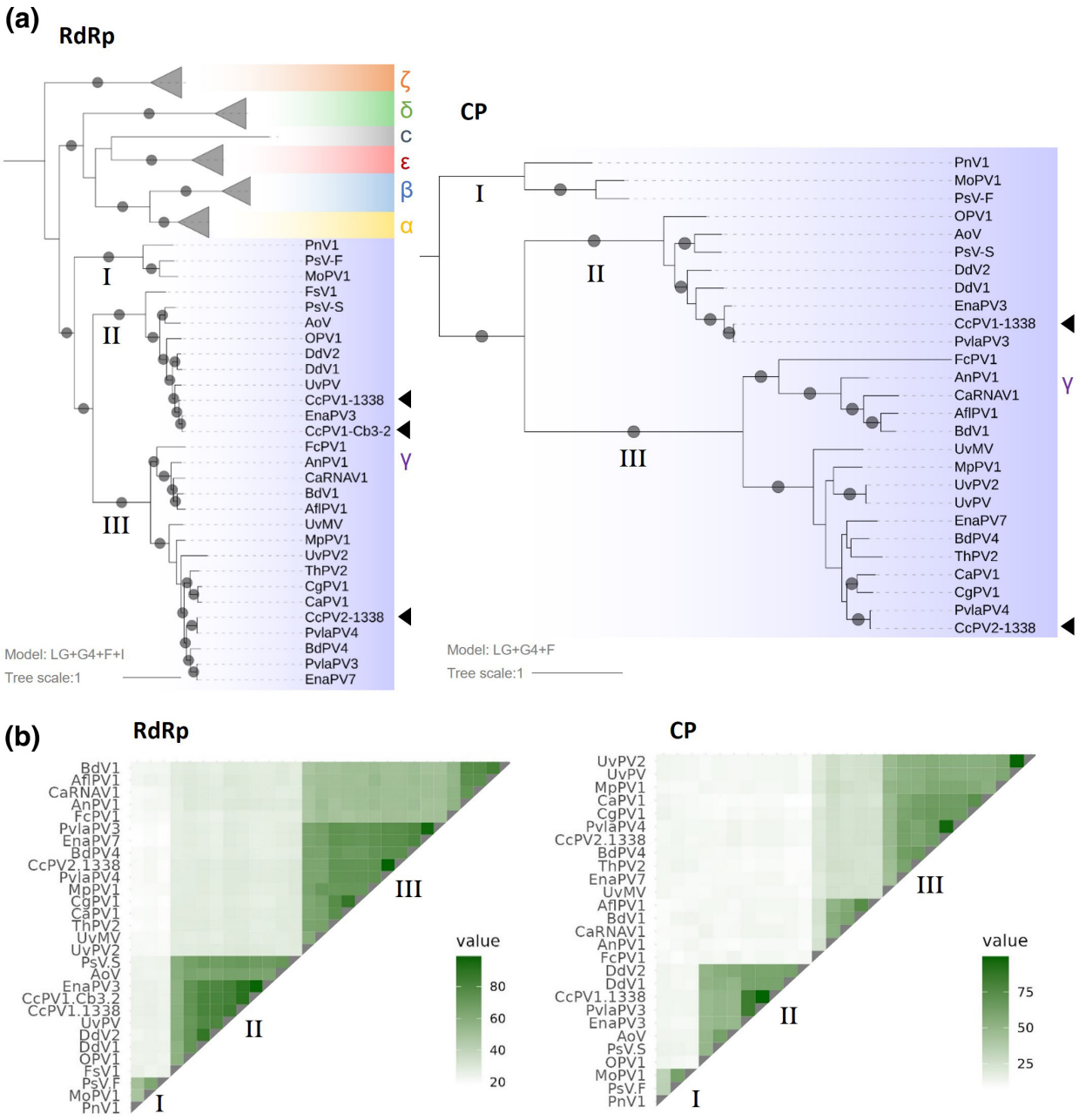

Fig. 5. Phylogenetic tree and pairwise identity matrix of RdRp and CP proteins. (a) Baesian maximum likelihood phylogenetic tree. Bootstrap support values greater than 70% are indicated on the branches by a grey circle. The left tree was built with LG+F+I+G4 model with a selection of RdRp sequences of Partitiviridae family (Table S2). HBPV was used as an outgroup. The tree on the right was built with LG+G4+F model with a selection of CP sequences of the *Gammapartitivirus* family and blastx hits of CP-CcPV1 and -CcPV2. The tree was rooted according to the RdRp phylogenetic tree. (b) Percentage of protein sequence identity with representative members of the *Gammapartitivirus* genus and blastx hits of CP-CcPv1 and -CcPV2 for which RdRp was also available. The numerical values of the matrix are given in Tables S4 and S5.

A typical and complete genomic structure of *Partitiviridae* was reconstructed for CcPV1. The association of the two fragments of this multipartite virus was based on the structure and size of the genome as well as with sequence similarity with members of the genus, the ORF of RNA1-1338 (i.e. contig1) being a polymerase and the ORF of RNA2-1338 (i.e. contig2) a coat protein [58]. The ends of the 5′ and 3′ untranslated regions of the RNA1 and 2 of CcPV1 showed strong sequence identity over more than 40 nucleotides, indicating that these are two genomic segments of the same virus. The RNA1 of the CcPV1 isolate from *C. ramotenellum* (Cb3.2) and the RNA1 of the CcPV1 isolate from *C. cladosporioides* (1338) shared 40/45 (88%) and 36/42 (86%) nucleotides at the 5′ and 3′ end respectively, in line with the percentage of identity of the RNA1 coding sequence

(91% aa). The two genomic segments RNA1 and 2 of CcPV2 also shared highly conserved 3′ and 5′-UTR, allowing their unambiguous association (Fig. 1). Despite the lack of functional annotation of ORF from RNA2 resulting from blastx analysis and CD search, determination of the protein sequence of the p41 protein isolated on an acrylamide gel following purification of CcPV2 virus particles by ultracentrifugation demonstrates its role as a structural protein. This role is also supported by the structure prediction performed with AlphaFold2 based on the amino acid sequence (Fig. 4). These predictions identify secondary and tertiary structures that support a functional proximity between the protein encoded by CcPV2 RNA2 and the CcPV1 capsid protein, despite their sequence divergence. Beyond the work presented in this article, this approach confirms its promising interest in proposing a function for the many proteins of mycoviruses whose function is unknown. This result provides experimental support for the assignment of a structural function to 15 closely related NCBI virus sequences that were previously annotated as hypothetical proteins or annotated CP with no experimental support.

This functional assignment extends the reach of this work to the taxonomic classification of the *Gammapartitivirus* genus by adding a new clade, consisting of CcPV-2 and 15 hitherto unclassified viruses. This clade showed high levels of genetic diversity for both RdRps and CPs, down to 19 and 9%, respectively, with the most distant members of the genus. The percentage of identity for the RdRp between members of the new clade (III) and the original clade (I) is below the 24% threshold set for the genus demarcation criteria, but stands above this threshold when compared with viruses of clade II. The size of the CP is also below the range observed in *Gammapartitivirus*. However, the grouping of these viruses into a new genus of *Partitiviridae* would break the existing monophyletic structure of the *Gammapartitivirus* group. Therefore, we recommend that the genus delimitation criteria for this viral family be modified to allow the incorporation of these 16 isolates representing 14 to 16 new species from the additional clade within the genus *Gammapartitivirus*. The distinction of two clades within *Gammapartitivirus* has recently been proposed by Wang *et al.* [41]. However, taking into account the above considerations and the specificity of this new capsid, which differs significantly from the capsids of the viruses assigned to clade I or II of the genus *Gammapartitivirus*, we propose the creation of a subgenus that brings together the 16 viruses of clade III presented in this work.

The high concordance of phylogenies based on RdRp sequences on one hand and on CP sequences on the other highlights two inconsistencies for UvPV and PvlaPV3. PvlaPV3 was identified in a metagenomic study. In the absence of biologically available isolates and RACE-PCR data to compare the complete ends of the fragments, it is not possible to verify whether this inconsistency is an incorrect association of segments from two distinct viruses or cases of reassortment. UvPV is an interesting case prepared from a pure culture of a *Ustilaginoidea virens* strain maintained in a collection and containing four viral genomic fragments. The first two fragments associated by 5′ end analysis correspond to a group II RdRp and CP. The third fragment – unfortunately incomplete at its ends – clustered in the new clade III of *Gammapartitiviruses*. Further work is required to verify whether these are two distinct viruses for which an RdRp is missing, or whether this third fragment is a form of virus that is a satellite of the first.

The characterisation of the CcPV2 genome also reveals an exceptionally long conserved region spanning 69/74 nucleotides of the 3′ UTR, which was almost the entire non-coding area of RdRp (84 nt) and a large part of the non-coding area of CP (118 nt). This long-conserved region of CcPV2 has no homology to any other virus. Highly conserved UTR of segments of multipartite virus have previously been observed in viruses of different families and may extend to the entire untranslated sequence [59–61]. However, in the *Partitiviridae* family, the conserved motif was so far short, restricted to a few nucleotides of the untranslated ends with some genus specificity [50, 62] although it sometimes extended beyond these few nucleotides [63, 64].

The role of high conservation level of UTRs remains to be defined, but similar to the role proposed for segmented viruses [65–67], it may ensure packaging and transcriptional specificity to limit reassortment. Thus, this high degree of specificity of the untranslated ends that distinguishes these two viral species, most likely contributes to the stability of their coexistence within the same fungal strain over the last 12 years.

CONCLUSION

The identification of a new form of capsid within the Gamma partitiviruses has led to the inclusion of 16 previously unassigned viruses in this viral family. These viruses form a new group that is clearly distinct from the other viruses in this genus.

This work has prompted us to propose the creation of a subgenus within the Gamma partitiviruses.

Funding information
This work received no specific grant from any funding agency

Acknowledgements
We would like to thank François Maclot for his precious advices for VANA extraction. We are grateful to Nicole Lecoultre and Emilie Michellod who helped in the fungal community construction. We are also grateful to Arnaud Blouin for his careful review of the manuscript.

Author contributions

A.J.: Conceptualization, Methodology, Formal analysis, Investigation, Writing - original draft, Visualization. N.D.: Investigation. I.K.: Investigation. J.B.: Investigation. S.S.: Writing - review & editing. K.G.: Writing - review & editing. O.S.: Conceptualization, Writing - original draft, Writing - review & editing, Supervision, Project administration, Funding acquisition

Conflicts of interest

The authors have no conflicts of interest.

References

1. Porras-Alfaro A, Bayman P. Hidden fungi, emergent properties: endophytes and microbiomes. *Annu Rev Phytopathol* 2011;49:291–315.
2. Belda I, Zarraonaindia I, Perisin M, Palacios A, Acedo A. From vineyard soil to wine fermentation: microbiome approximations to explain the "terroir" concept. *Front Microbiol* 2017;8:821.
3. Kashif M, Jurvansuu J, Vainio EJ, Hantula J. Alphapartitiviruses of *Heterobasidion w*ood decay fungi affect each other's transmission and host growth. *Front Cell Infect Microbiol* 2019;9.
4. Knowlton N, Rohwer F. Multispecies microbial mutualisms on coral reefs: the host as a habitat. *Am Nat* 2003;162:S51–S62.
5. Nerva L, Garcia JF, Favaretto F, Giudice G, Moffa L, *et al*. The hidden world within plants: metatranscriptomics unveils the complexity of wood microbiomes. *J Exp Bot* 2022;73:2682–2697.
6. Terhonen E, Blumenstein K, Kovalchuk A, Asiegbu FO. Forest tree microbiomes and associated fungal endophytes: functional roles and impact on forest health. *Forests* 2019;10:42.
7. Vandenkoornhuyse P, Quaiser A, Duhamel M, Le Van A, Dufresne A. The importance of the microbiome of the plant holobiont. *New Phytol* 2015;206:1196–1206.
8. Pacifico D, Squartini A, Crucitti D, Barizza E, Lo Schiavo F, *et al*. The role of the endophytic microbiome in the grapevine response to environmental triggers. *Front Plant Sci* 2019;10.
9. Nuss DL. Biological control of chestnut blight: an example of virus-mediated attenuation of fungal pathogenesis. *Microbiol Rev* 1992;56:561–576.
10. Rigling D, Prospero S. Cryphonectria parasitica, the causal agent of chestnut blight: invasion history, population biology and disease control. *Mol Plant Pathol* 2017;19:7–20.
11. Zhang H, Xie J, Fu Y, Cheng J, Qu Z, *et al*. A 2-kb mycovirus converts a pathogenic fungus into a beneficial endophyte for brassica protection and yield enhancement. *Mol Plant* 2020;13:1420–1433.
12. Al Rwahnih M, Daubert S, Urbez-Torres JR, Cordero F, Rowhani A. Deep sequencing evidence from single grapevine plants reveals a virome dominated by mycoviruses. *Arch Virol* 2011;156:397–403.
13. Chiapello M, Rodríguez-Romero J, Ayllón MA, Turina M. Analysis of the virome associated to grapevine downy mildew lesions reveals new mycovirus lineages. *Virus Evol* 2020;6:veaa058.
14. Pandey B, Naidu RA, Grove GG. Detection and analysis of mycovirus-related RNA viruses from grape powdery mildew fungus Erysiphe necator. *Arch Virol* 2018;163:1019–1030.
15. Bensch K, Groenewald JZ, Braun U, Dijksterhuis J, Starink M, *et al*. Biodiversity in the cladosporium herbarum complex (davidiellaceae, capnodiales), with standardisation of methods for cladosporium taxonomy and diagnostics. *Stud Mycol* 2007;58:105–156.
16. Deyett E, Rolshausen PE. Temporal dynamics of the sap microbiome of grapevine under high pierce's disease pressure. *Front Plant Sci* 2019;10:1246.
17. Nerva L, Turina M, Zanzotto A, Gardiman M, Gaiotti F, *et al*. Isolation, molecular characterization and virome analysis of culturable wood fungal endophytes in esca symptomatic and asymptomatic grapevine plants. *Environ Microbiol* 2019;21:2886–2904.
18. Liu D, Howell K. Community succession of the grapevine fungal microbiome in the annual growth cycle. *Environ Microbiol* 2021;23:1842–1857.
19. Briceño EX, Latorre BA. Characterization of cladosporium rot in grapevines, a problem of growing importance in Chile. *Plant Dis* 2008;92:1635–1642.
20. Hofstetter V, Buyck B, Croll D, Viret O, Couloux A, *et al*. What if esca disease of grapevine were not a fungal disease? *Fungal Diversity* 2012;54:51–67.
21. Pilotti M, Faggioli F, Barba M. Characterization of italian isolates of pear vein yellows virus. In: *Acta Horticulturae*. Leuven, Belgium: International Society for Horticultural Science (ISHS), 1995. pp. 148–154.
22. Mahillon M, Brodard J, Kellenberger I, Blouin AG, Schumpp O. A novel weevil-transmitted tymovirus found in mixed infection on hollyhock. *Virol J* 2023;20:17.
23. Akbergenov R, Si-Ammour A, Blevins T, Amin I, Kutter C, *et al*. Molecular characterization of geminivirus-derived small RNAs in different plant species. *Nucleic Acids Res* 2006;34:462–471.
24. Candresse T, Filloux D, Muhire B, Julian C, Galzi S, *et al*. Appearances can be deceptive: revealing a hidden viral infection with deep sequencing in a plant quarantine context. *PLoS One* 2014;9:e102945.
25. Filloux D, Dallot S, Delaunay A, Galzi S, Jacquot E, *et al*. Metagenomics approaches based on virion-associated nucleic acids (VANA): an innovative tool for assessing without a priori viral diversity of plants. In: Lacomme C (ed). *Plant Pathology: Techniques and Protocols*. New York, NY: Springer. pp. 249–257.
26. Maclot FJ, Debue V, Blouin AG, Fontdevila Pareta N, Tamisier L, *et al*. Identification, molecular and biological characterization of two novel secovirids in wild grass species in Belgium. *Virus Res* 2021;298:198397.
27. Bankevich A, Nurk S, Antipov D, Gurevich AA, Dvorkin M, *et al*. SPAdes: a new genome assembly algorithm and its applications to single-cell sequencing. *J Comput Biol* 2012;19:455–477.
28. BBDuk Guide. DOE Joint Genome Institute; (n.d.). https://jgi.doe.gov/data-and-tools/software-tools/bbtools/bb-tools-user-guide/bbduk-guide/ [accessed 5 June 2020].
29. Asamizu T, Summers D, Motika MB, Anzola JV, Nuss DL. Molecular cloning and characterization of the genome of wound tumor virus: a tumor-inducing plant reovirus. *Virology* 1985;144:398–409.
30. Abràmoff DMD. Image Processing with ImageJ; 2004 Jul. https://imagej.nih.gov/ij/docs/pdfs/Image_Processing_with_ImageJ.pdf
31. Ahmed I, Li P, Zhang L, Jiang X, Bhattacharjee P, *et al*. First report of a novel partitivirus from the phytopathogenic fungus fusarium cerealis in China. *Arch Virol* 2020;165:2979–2983.
32. Nerva L, Silvestri A, Ciuffo M, Palmano S, Varese GC, *et al*. Transmission of *Penicillium aurantiogriseum* partiti-like virus 1 to a new fungal host (*Cryphonectria parasitica*) confers higher resistance to salinity and reveals adaptive genomic changes. *Environ Microbiol* 2017;19:4480–4492.
33. Edgar RC. MUSCLE: multiple sequence alignment with high accuracy and high throughput. *Nucleic Acids Res* 2004;32:1792–1797.
34. Kalyaanamoorthy S, Minh BQ, Wong TKF, von Haeseler A, Jermiin LS. ModelFinder: fast model selection for accurate phylogenetic estimates. *Nat Methods* 2017;14:587–589.
35. Trifinopoulos J, Nguyen L-T, von Haeseler A, Minh BQ. W-IQ-TREE: a fast online phylogenetic tool for maximum likelihood analysis. *Nucleic Acids Res* 2016;44:W232–W235.
36. Hoang DT, Chernomor O, von Haeseler A, Minh BQ, Vinh LS. UFBoot2: improving the ultrafast bootstrap approximation. *Mol Biol Evol* 2018;35:518–522.
37. Ciccarelli FD, Doerks T, von Mering C, Creevey CJ, Snel B, *et al*. Toward automatic reconstruction of a highly resolved tree of life. *Science* 2006;311:1283–1287.

38. El-Gebali S, Mistry J, Bateman A, Eddy SR, Luciani A, *et al*. The pfam protein families database in 2019. *Nucleic Acids Res* 2019;47:D427–D432.
39. Starr EP, Nuccio EE, Pett-Ridge J, Banfield JF, Firestone MK. Metatranscriptomic reconstruction reveals RNA viruses with the potential to shape carbon cycling in soil. *Proc Natl Acad Sci*2019;116:25900–25908.
40. Vainio EJ, Chiba S, Ghabrial SA, Maiss E, Roossinck M, *et al*. ICTV virus taxonomy profile: partitiviridae. *J Gen Virol* 2018;99:17–18.
41. Wang P, Yang G, Shi N, Zhao C, Hu F, *et al*. A novel partitivirus orchestrates conidiation, stress response, pathogenicity, and secondary metabolism of the entomopathogenic fungus metarhizium majus. *PLoS Pathog* 2023;19:e1011397.
42. Wang J, Youkharibache P, Zhang D, Lanczycki CJ, Geer RC, *et al*. iCn3D, a web-based 3D viewer for sharing 1D/2D/3D representations of biomolecular structures. *Bioinformatics* 2020;36:131–135.
43. Ochoa WF, Havens WM, Sinkovits RS, Nibert ML, Ghabrial SA, *et al*. Partitivirus structure reveals a 120-subunit, helix-rich capsid with distinctive surface arches formed by quasisymmetric coat-protein dimers. *Structure* 2008;16:776–786.
44. Chun J, Ko Y-H, Kim D-H. Transcriptome analysis of *Cryphonectria parasitica* infected with cryphonectria hypovirus 1 (CHV1) reveals distinct genes related to fungal metabolites, virulence, antiviral RNA-silencing, and their regulation. *Front Microbiol* 2020;11:1711.
45. Lemus-Minor CG, Cañizares MC, García-Pedrajas MD, Pérez-Artés E. Fusarium oxysporum f. sp. dianthi virus 1 accumulation Is correlated with changes in virulence and other phenotypic traits of its fungal host. *Phytopathology* 2018;108:957–963.
46. Xiao X, Cheng J, Tang J, Fu Y, Jiang D, *et al*. A novel partitivirus that confers hypovirulence on plant pathogenic fungi. *J Virol* 2014;88:10120–10133.
47. Ahn I-P, Lee Y-H. A viral double-stranded RNA up regulates the fungal virulence of Nectria radicicola. *MPMI* 2001;14:496–507.
48. Bhatti MF, Jamal A, Petrou MA, Cairns TC, Bignell EM, *et al*. The effects of dsRNA mycoviruses on growth and murine virulence of Aspergillus fumigatus. *Fungal Genet Biol* 2011;48:1071–1075.
49. Filippou C, Diss RM, Daudu JO, Coutts RHA, Kotta-Loizou I. The polymycovirus-mediated growth enhancement of the entomopathogenic fungus *Beauveria bassiana* is dependent on carbon and nitrogen metabolism. *Front Microbiol* 2021;12:606366.
50. Gilbert KB, Holcomb EE, Allscheid RL, Carrington JC. Hiding in plain sight: new virus genomes discovered via a systematic analysis of fungal public transcriptomes. *PLoS One* 2019;14:e0219207.
51. Kamaruzzaman M, He G, Wu M, Zhang J, Yang L, *et al*. A novel partitivirus in the hypovirulent isolate QT5-19 of the plant pathogenic fungus botrytis cinerea. *Viruses* 2019;11:24.
52. Zheng L, Zhang M, Chen Q, Zhu M, Zhou E. A novel mycovirus closely related to viruses in the genus alphapartitivirus confers hypovirulence in the phytopathogenic fungus *Rhizoctonia solani*. *Virology* 2014;456–457:220–226.
53. Latorre BA, Briceño EX, Torres R. Increase in cladosporium spp. populations and rot of wine grapes associated with leaf removal. *Crop Protection* 2011;30:52–56.
54. McHale MT, Roberts IN, Noble SM, Beaumont C, Whitehead MP, *et al*. CfT-I: an LTR-retrotransposon in cladosporium fulvum, a fungal pathogen of tomato. *Mol Gen Genet* 1992;233:337–347.
55. Maheshwari R, Navaraj A. Senescence in fungi: the view from Neurospora. *FEMS Microbiol Lett* 2008;280:135–143.
56. Maas MF, Debets AJ, Zwaan BJ. 17 why some fungi senesce and others do not. In: *The Evolution of Senescence in the Tree of Life*, vol. 341. 2017.
57. Vainio EJ, Jurvansuu J, Hyder R, Kashif M, Piri T, *et al*. Heterobasidion partitivirus 13 mediates severe growth debilitation and major alterations in the gene expression of a fungal forest pathogen. *J Virol* 2018;92:e01744-17.
58. Bozarth RF, Wood HA, Mandelbrot A. The Penicillium stoloniferum virus complex: two similar double-stranded RNA virus-like particles in a single cell. *Virology* 1971;45:516–523.
59. Chiba S, Salaipeth L, Lin Y-H, Sasaki A, Kanematsu S, *et al*. A novel bipartite double-stranded RNA mycovirus from the white root rot fungus rosellinia necatrix: molecular and biological characterization, taxonomic considerations, and potential for biological control. *J Virol* 2009;83:12801–12812.
60. Wu M, Jin F, Zhang J, Yang L, Jiang D, *et al*. Characterization of a novel bipartite double-stranded RNA mycovirus conferring hypovirulence in the phytopathogenic fungus botrytis porri. *J Virol* 2012;86:6605–6619.
61. Liu L, Wang Q, Cheng J, Fu Y, Jiang D, *et al*. Molecular characterization of a bipartite double-stranded RNA virus and its satellite-like RNA co-infecting the phytopathogenic fungus sclerotinia sclerotiorum. *Front Microbiol* 2015;6:406.
62. Nibert ML, Ghabrial SA, Maiss E, Lesker T, Vainio EJ, *et al*. Taxonomic reorganization of family partitiviridae and other recent progress in partitivirus research. *Virus Res* 2014;188:128–141.
63. Wang Y, Zhao H, Cao J, Yin X, Guo Y, *et al*. Characterization of a novel mycovirus from the phytopathogenic fungus Botryosphaeria dothidea. *Viruses* 2022;14:331.
64. Hamim I, Urayama S-I, Netsu O, Tanaka A, Arie T, *et al*. Discovery, genomic sequence characterization and phylogenetic analysis of novel RNA viruses in the turfgrass pathogenic *Colletotrichum* spp. in Japan. *Viruses* 2022;14:2572.
65. Robertson JS. 5' and 3' terminal nucleotide sequences of the RNA genome segments of influenza virus. *Nucleic Acids Res* 1979;6:3745–3757.
66. McDonald SM, Nelson MI, Turner PE, Patton JT. Reassortment in segmented RNA viruses: mechanisms and outcomes. *Nat Rev Microbiol* 2016;14:448–460.
67. Gao Q, Palese P. Rewiring the RNAs of influenza virus to prevent reassortment. *Proc Natl Acad Sci*2009;106:15891–15896.